HETEROCYCLES, Vol. 104, No. 7, 2022, pp. 1280 - 1292. © 2022 The Japan Institute of Heterocyclic Chemistry
Received, 11th April, 2022, Accepted, 13th May, 2022, Published online, 18th May, 2022
DOI: 10.3987/COM-22-14672

NEW DIMERIC CYTISINE-TYPE ALKALOID AND LAVANDULYL BIFLAVONOID FROM *SOPHORA FLAVESCENS* AIT. AND THEIR INHIBITORY EFFECT ON CANCER CELLS

Shengxue Chen,[1#] Yan Liu,[1] Chenting Meng,[1] Min Li,[1] Chunping Yuan,[1,2] and Xiaoying Yin[1,2,3]*

[1]School of Chemistry and Chemical Engineering, Shanghai University of Engineering Science, Shanghai, 201620, China; [2]Shanghai Engineering Research Center for Pharmaceutical Intelligent Equipment, Shanghai University of Engineering Science, Shanghai, 201620, China; [3]Shanghai Frontiers Science Research Center for Druggability of Cardiovascular noncoding RNA, Institute for Frontier Medical Technology, Shanghai University of Engineering Science, Shanghai, 201620, China; [#]First author: sxchen1009@163.com, *Corresponding author: ncyxoy@163.com.

Abstract – Two new dimeric compounds with antitumor activity were extracted for the first time from *Sophora flavescens* Ait. using several chromatographic separation methods. Compound **1** (sophobikushenine) is a dimeric cytisine-type alkaloid connected by an eight-membered heterocycle ring, and compound **2** (sophobiflavanone) is a lavandulyl biflavonoid consisting of a skeleton including nitrogen atoms as heteroatoms. The structures of the two compounds were elucidated using one- and two-dimensional NMR, ECD, and HR-ESI-MS. The inhibitory effects of the new compounds against A431 and BT474 were evaluated *in vitro* implementing CCK-8 and scratch assays. Sophobiflavanone inhibited the growth of A431 cells with an IC_{50} value of 37.77 ± 0.98 μM and BT474 cells with an IC_{50} value of 38.13 ± 0.31 μM; further, it exhibited a strong antimigratory activity toward 4T1.

INTRODUCTION

Sophora flavescens (S. flavescens), which is known as "Kushen" in China, belongs to the Leguminosae family and is widely distributed across China, particularly in Hebei and Henan.[1] The dried roots of *S. flavescens*, which are called *S. flavescens* Ait., are used clinically in traditional Chinese medicine to treat

cancer, inflammation, and eczema.[2] The results of pharmacological investigations indicate that *S. flavescens* Ait. exhibits considerable antibacterial [3]and antiviral activity against hepatitis B virus,[4] as well as potent and selective inhibitory activity of cancer cells,[5] which makes *S. flavescens* Ait. worthy of further research.

The major bioactive components of *S. flavescens* Ait. are alkaloids and flavonoids. According to phytochemical studies, more than 50 alkaloids and 100 flavonoids have been isolated from the plant.[6] Besides these monomeric compounds, since 2016, researchers have extracted 14 dimeric compounds from *S. flavescens* Ait.[7,8] These dimeric compounds could be divided into two types: dimerized alkaloids and dimerized flavonoids. Compared with their monomeric counterparts, some dimeric compounds can improve the efficacy toward cancer targets as well as the overall efficacy.[9] Dimeric compounds are developed as antitumor drug candidates because they have the potential to bind two sites on a single receptor or to the target sites of two monomers in a dimeric protein.[10] Numerous well-known targets for anticancer therapy, including protein signaling[11] and DNA topoisomerases,[12] dimerize or require dimerization for activation. Therefore, developing dimeric and multivalent antitumor inhibitory drugs is an important research goal.

In this study, the following two compounds were isolated from *S. flavescens* Ait. and structurally characterized (Figure 1) using 1D and 2D NMR spectroscopy, ECD, and HR-ESI-MS: sophobikushenine (**1**), the first natural cytisine-type alkaloid dimer, and sophobiflavanone (**2**), which is the product of an unprecedented dimerization between two lavandulyl flavonoids containing nitrogen as heteroatoms. The cytotoxic effects of these two compounds on A431, human skin squamous cancer cells, and BT474, breast cancer cells, as well as cell migration of 4T1, mouse breast cancer cells, were evaluated. Here, the isolation, structural elucidation and inhibitory activity of cancer cells of these compounds are described.

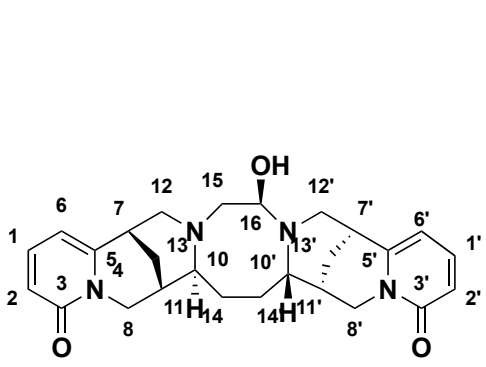

Sophobikushenine
1

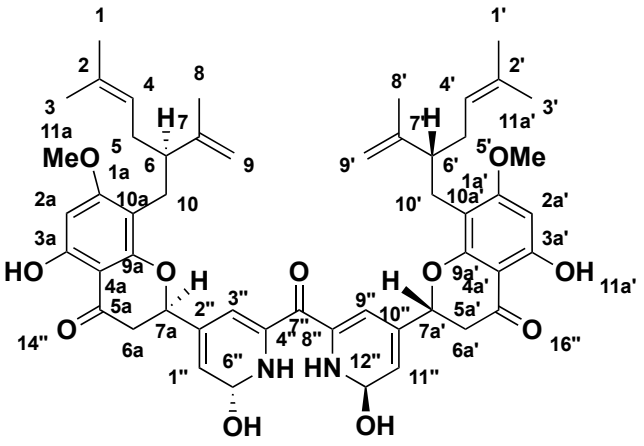

Sophobiflavanone
2

Figure 1. Chemical structures of compounds **1**–**2** from *Sophora flavescens* Ait.

RESULTS AND DISCUSSION

Compound identification Compound **1** was isolated as a yellow oil. The molecular formula of **1** was deduced to be $C_{26}H_{32}N_4O_3$, based on the observed HR-ESI-MS peak at *m/z* 471.2378 [M + Na] + (calcd for $C_{26}H_{32}N_4O_3Na$: 471.2372). Notably, this molecular formula implies 13 degrees of unsaturation for compound **1**. The IR spectroscopy absorption bands at 3413, 2928, 1646, and 1584 cm^{-1} indicated N–H groups, hydroxyl groups, carbonyl groups, and C=C bonds, respectively.

The ^{13}C NMR spectrum of **1** included resonance peaks owing to 26 carbons, including two peaks owing to carbonyls, at δ_C 165.5 (C-3) and 165.8(C-3′), and eight peaks owing to carbon centers involved in C=C bonding interactions, at δ_C 107.7 (C-6), 108.1 (C-6′), 116.6 (C-2), 116.8 (C-2′), 141.2 (C-1), 141.3 (C-1′), 153.9 (C-5), and 153.0 (C-5′). Further, we found that most of these carbon spectrum data appear in pairs and are consistent with the cytisine-type data.[13] In the ^1H NMR spectrum of compound **1**, the proton signals owing to six adjacent aromatic hydrogens, at δ_H 6.26 (1H, d, *J* = 7.1 Hz, H-6), 6.28 (1H, d, *J* = 7.0 Hz, H-6′), 6.38 (1H, d, *J* = 8.9, 1.3 Hz, H-2), 6.41 (1H, d, *J* = 8.9, 1.4 Hz, H-2′), 7.44–7.42 (1H, m, H-1), and 7.47–7.45 (1H, m, H-1′), were assigned to a pyridone ring on the cytisine-type skeleton. Further, δ_H 2.47 (1H, d, *J* = 11.0 Hz, H-12), 3.92 (1H, d, *J* = 6.6 Hz, H-12), 4.05 (1H, d, *J* = 15.6 Hz, H-12′), 3.90–3.87 (1H, m, H-12′) were the characteristic peaks hydrogen signal of H12/H12′ on cytisine-type alkaloids.[14] After assigning the ^1H NMR and ^{13}C NMR resonance signals to a cytisine-type compound, a number of several ^1H NMR signals remained unassigned: δ_H 1.95–1.91 (2H, m, H-14), 2.21 (1H, td, *J* = 13.4, 2.9 Hz, H-14′), 1.28–1.24 (1H, m, H-14′), 2.40 (1H, dd, *J* = 13.8, 4.4 Hz, H-15), 3.22 (1H, td, *J* = 13.9, 3.0 Hz, H-15), and 4.18–4.17 (1H, m, H-16); We interpreted these data by considering that two cytisine-type compounds may be connected by a ring. This conclusion was confirmed by the presence of HMBC correlations between H-15 (δ_H 2.40, 1H, dd, *J* = 13.8, 4.4 Hz) and C-10 (δ_C 57.3), H-15 (δ_H 2.40, 1H, dd, *J* = 13.8, 4.4 Hz) and C-16 (δ_C 66.3), H-14′ (δ_H 2.21, 1H, td, *J* = 13.4, 2.9 Hz) and C-10 (δ_C 57.3). The ^1H–^1H COSY correlations of H-1/H-2/H-6, H-10/H-14/H-14′, H-1′/H-2′/H-6′, H-8/H-11 and H-11/H-13a indicated the presence of four isolated spin systems. The relative configuration of compound **1** was determined by using analysis of the NOESY correlations of this compound and the ^1H NMR spectroscopic coupling constants. In the NOESY spectrum of **1**, the existence of correlations between H-13′ (δ_H 1.24–1.21, 1H, m) and H-14′ (δ_H 2.21 1H, td, *J* = 13.4, 2.9 Hz) as well as H-14 (δ_H 1.95–1.91, 2H, m), together with the lack of any observed correlations between H-13 and H-14, H-14′, implied that H-13′ and H-14, H-14′ have the same orientation, but H-13 and H-14, H-14′ have different orientations. With the aid of using 2D NMR experiments, including ^1H–^1H COSY, HSQC, HMBC, and NOESY (Figure 2a), all the ^1H and ^{13}C NMR resonance peaks of **1** were assigned (Table 1).

The absolute configurations of C-10, C-10′ and C-16 in **1** were established by comparing its experimental ECD spectrum to the calculated ECD spectra. The lowest energy conformations of **1** were obtained by a

systematic conformational analysis using MMFF94 molecular mechanics force field calculations. The theoretical ECD spectrum was calculated using time-dependent density functional theory (TD-DFT) at the B3LYP/6-311+G (d, p) level. As shown in Figure 3a, the calculated ECD curve of (10s,10′s,16R)-**1** was in good agreement with the experimental spectrum of **1**, which allowed us to assign the absolute configuration of **1** as 10*S*,10′*S*,16*R*. Consequently, the structure of **1** was determined to be as shown, and the compound **1** was named sophobikushenine.

Table 1. NMR data for sophobikushenine **1**

Position	δ_C[1]	δ_H[2]
1	141.2	7.44 – 7.42 (1H, m)
2	116.6	6.38 (1H, d, *J* = 8.9, 1.3 Hz)
3	165.5	–
5	153.9	–
6	107.7	6.26 (1H, d, *J* = 7.1 Hz)
7	36.4	3.08 – 3.06 (1H, m)
8	53.1	4.00 (1H, d, *J* =15.4 Hz) 3.45-3.44 (1H, m)
10	57.3	3.41 – 3.39 (1H, m)
11	33.3	2.14 – 2.09 (1H, m)
12	53.2	2.47 (1H, d, *J* = 11.0 Hz) 3.92 (1H, d, *J* = 6.6 Hz)
13	21.0	1.71 (1H, dd, *J* = 13.3, 2.7 Hz) 2.05 (1H, dd, *J* = 13.4, 3.3 Hz)
14	26.6	1.95 – 1.91 (2H, m)
15	49.0	2.40 (1H, dd, *J* = 13.8, 4.4 Hz) 3.22 (1H, td, *J* = 13.9, 3.0 Hz)
16	66.3	4.18 – 4.17 (1H, m)
1′	141.3	7.47 – 7.45 (1H, m)
2′	116.8	6.41 (1H, d, *J* = 8.9, 1.4 Hz)
3′	165.8	–
5′	153.0	–
6′	108.1	6.28 (1H, d, *J* = 7.0 Hz)
7′	36.6	3.04 – 3.03 (1H, m)
8′	54.1	3.02 – 2.99 (1H, m) 3.42 – 3.40 (1H, m)
10′	52.9	2.96 – 2.94 (1H, m)
11′	28.8	2.35-2.32 (1H, m)
12′	51.1	4.05 (1H, d, *J* = 15.6 Hz)

		3.90 – 3.87 (1H, m)
13′	26.1	1.24 – 1.21 (1H, m)
		1.99 (1H, d, *J* = 3.4 Hz)
14′	29.7	2.21 (1H, td, *J* = 13.4, 2.9 Hz)
		1.28 – 1.24 (1H, m)

[1] 125 MHz, δ in ppm, *J* in Hz. Data recorded in Methanol-*d*$_4$.

[2] 500 MHz, δ in ppm, *J* in Hz. Data recorded in Methanol-*d*$_4$.

Compound **2** was isolated as a yellow amorphous powder, which exhibited the typical flavonoid skeleton UV absorption pattern, with maxima at 238 and 291 nm. The molecular formula of **2** was $C_{51}H_{60}N_2O_{11}$ based on the observed HR-ESI-MS peak at *m/z* 899.4101 [M + Na] + (calculated for $C_{51}H_{60}N_2O_{11}$ Na: 899.4095). The IR spectrum of **2** included absorption bands attributable to conjugated carbonyls (1599 cm^{-1}), and aromatic rings (1499 and 1459 cm^{-1}).

The ^{1}H NMR spectrum of **2** comprised eight singlet aromatic protons at δ_H 7.21 (1H, d, *J* = 2.3 Hz, H-11″), 7.22 (1H, d, *J* = 2.3 Hz, H-1″), 6.25 (1H, t, *J* = 2.3 Hz, H-12″), 6.26 (1H, t, *J* = 2.3 Hz, H-6″), 6.33 (1H, s, H-3″), 6.33 (1H, overlap, H-9″), 6.11 (1H, s, H-2a), 6.11 (1H, overlap, H-2a′), which were owing to tetrasubstituted or pentasubstituted benzene rings; there are also comprised diagnostic flavonoid signals at δ_H 5.43 (1H, dd, *J* = 13.2, 2.7 Hz, H-7a), 5.37 (1H, dd, *J* = 13.2, 2.7 Hz, H-7a′), 2.46 – 2.45(1H, m, H-6a), 2.84 – 2.81 (1H, m, H-6a), 2.80–2.76 (1H, m, H-6a′), and 2.45–2.43 (1H, m, H-6a′). In addition, two resonance signals owing to protons in methoxy groups at δ_H 3.70 (3H, s, OMe-11a) and 3.70 (3H, overlap, OMe-11a′) and two sets of signals owing to the lavandulyl group at δ_H [1.43 (3H, s, H-1), 1.49 (3H, s, H-1′), 1.58 (3H, s, H-8), 1.51 (3H, s, H-8′), 1.56 (3H, s, H-3), 1.53 (3H, s, H-3′), 2.50–2.49 (2H, m, H-10), 2.49–2.47 (2H, m, H-10′), 2.02–1.97 (1H, m, H-5), 1.93–1.87 (1H, m, H-5), 1.97–1.93 (2H, m, H-5′), 2.42–2.39 (1H, m, H-6), 2.39–2.35 (1H, m, H-6′), 4.55−4.52 (1H, m, H-9), 4.48 (1H, d, *J* = 2.7 Hz, H-9), 4.52−4.51 (1H, m, H-9′), 4.38 (1H, d, *J* = 2.7 Hz, H-9′), 4.94 (1H, t, *J* = 6.9 Hz, H-4), and 4.90 (1H, t, *J* = 6.9 Hz, H-4′) were observed. Based on the characteristics of the ^{13}C NMR and ^{1}H NMR spectra of compound **2**, we assume that this compound is characterized by symmetry. The ^{13}C NMR and HSQC spectra of **2** comprised 51 carbon resonances, including 18 flavonoid skeleton carbons,[15] two carbons assignable to methoxy groups, and 20 carbons belonging to two lavandulyl groups. [16] The signals owing to the remaining 11 carbons at δ_C 179.6, 158.1, 158.1, 127.3, 127.2, 116.4, 116.6, 106.3, 106.3, 102.3, and 102.3 indicated a symmetric aromatic ring with a carbonyl.

^{1}H–^{1}H COSY correlations indicated six spin systems, namely, H-4/H-5, H-4′/H-5′, H-6a/H-7a, H-6a′/H-7a′, H-1″/H-6″ and H-11″/H-12″. Notably, the linkage through C7a–C2″ and C7a′–C10″ bonds of these two units, was unambiguously established based on the HMBC correlations between C-7a (δ_C

73.5) and H-1″ (δ_H 7.22, 1H, d, *J* = 2.3 Hz) as well as C-2″ (δ_C 116.4) and H-6aβ (δ_H 2.84 – 2.81, 1H, m), and between C-7a′ (δ_C 73.5) and H-11″ (δ_H 7.21, 1H, d, *J* = 2.3 Hz) as well as C-10″ (δ_C 116.6) and H-6a′ (δ_H 2.80–2.76, 1H, m). The HMBC cross peaks of MeO-11a (δ_H 3.70) with C-1a (δ_C 162.5) and MeO-11a″ (δ_H 3.70) with C-1a″ (δ_C 162.5) confirmed that the two methoxy groups were located at C-1a and C-1a″, respectively. Two lavandulyl groups exhibited HMBC correlations between H-10 (δ_H 2.50 – 2.49, 2H, m) and C-10a (δ_C 162.1) and between H-10′ (δ_H 2.49 – 2.47, 2H, m) and C-10a′ (δ_C 162.1) confirmed that the two lavandulyl groups were located at C-10a and C-10a′, respectively. The observation of four ^{13}C NMR resonance peaks attributable to oxygenated aromatic carbons indicated oxygen atoms at C-7a (δ_C 73.5), C-7a′ (δ_C 73.5), C-9a (δ_C 155.2), and C-9a′ (δ_C 155.3), as well as four hydroxyl groups located on benzene rings. Based on the described comprehensive spectroscopic analysis, compound **2** was determined to exhibit the structure reported in Figure 1, where the two monomers were identified as 3a, 6″-dihydroxy-10a-lavandulyl-1a-methoxy-5″-hydropyridine flavonoid and 3a′,12″-dihydroxy-2a′-lavandulyl-1a′-methoxy-13″-hydropyridine flavonoid, a biflavonoid linked via a C4″-C8″ carbonyl bond. In the NOESY spectra, we could observe H-8 (δ_H 1.58, 3H, s) on the lavender group is related to H-6"(δ_H 6.26, 1H, t, *J* = 2.3 Hz), and H-8 (δ_H 1.58, 3H, s) is related to H-1" (δ_H 7.22 1H, d, *J* = 2.3 Hz), indicating that the lavender group is spatially close to the center of symmetry. For clearly marked, we only show the NOESY correlations of one side of the symmetrical compound. With the aid of using 2D NMR experiments, including ^{1}H–^{1}H COSY, HSQC, HMBC and NOESY (Figure 2b), all ^{1}H and ^{13}C NMR resonance peaks of **2** were assigned (Table 2).

The absolute configuration of compound **2** was confirmed by comparison of calculated and experimental ECD spectra (Figure 3b). The experimental spectrum of **2** exhibited negative Cotton effect (CE) at 265 nm, and positive CE at 216, 372 nm, which agreed with the calculated spectrum of the (6*R*,6′*R*, 7a*R*,7a′*R*,6″*R*,12″*R*)-**2**. Therefore, the structure of **2** was finally elucidated and was named sophobiflavanone.

Table 2. NMR data for sophobiflavanone **2**

Position	δ_C[1]	δ_H[2]
1	17.6	1.43 (3H, s)
2	130.6	–
3	25.5	1.56 (3H, s)
4	123.4	4.94 (1H, t, *J* = 6.9 Hz)
5	30.7	2.02 – 1.97 (1H, m) 1.93 – 1.87 (1H, m)

6	46.4	2.42 – 2.39 (1H, m)
7	147.6	–
8	18.3	1.58 (3H, s)
9	110.7	4.55 – 4.52 (m, 1H) 4.48 (d, *J* = 2.7 Hz, 1H)
10	26.9	2.50 – 2.49 (2H, m)
1a	162.5	–
2a	92.4	6.11 (1H, s)
3a	104.3	–
4a	107	–
5a	188.9	–
6a	44.3	2.46 – 2.45 (1H, m) 2.84 – 2.81 (1H, m)
7a	73.5	5.43 (1H, dd, *J* = 13.2, 2.7 Hz)
9a	155.2	–
10a	162.1	–
11a	55.3	3.70 (3H, s)
1′	17.7	1.49 (3H, s)
2′	130.6	–
3′	25.6	1.53 (3H, s)
4′	123.4	4.90 (1H, t, *J* = 6.9 Hz)
5′	31	1.97 – 1.93 (2H, m)
6′	46.8	2.39 – 2.35 (1H, m)
7′	147.9	–
8′	18.6	1.51 (3H, s)
9′	110.7	4.52 – 4.51 (m, 1H) 4.38 (d, *J* = 2.7 Hz, 1H)
10′	27	2.49 – 2.47 (2H, m)
1a′	162.5	–
2a′	92.5	6.11 (1H, s)
3a′	104.3	–
4a′	107.1	–
5a′	189	–
6a′	44.5	2.45 – 2.43 (1H, m) 2.80 – 2.76 (1H, m)
7a′	73.5	5.37 (1H, dd, *J* = 13.2, 2.7 Hz)

9a′	155.3	–
10a′	162.1	–
11a′	55.3	3.70 (3H, s)
1″	127.2	7.22 (1H, d, *J* = 2.3 Hz)
2″	116.4	–
3″	102.3	6.33 (1H, s)
4″	158.1	–
6″	106.3	6.26 (1H, t, *J* = 2.3 Hz)
7″	179.6	–
8″	158.1	–
9″	102.3	6.33 (1H, s)
10″	116.6	–
11″	127.3	7.21 (1H, d, *J* = 2.3 Hz)
12″	106.3	6.25 (1H, t, *J* = 2.3 Hz)

[1] 125 MHz, δ in ppm, *J* in Hz. Data recorded in Dimethyl Sulfoxide-d_6.

[2] 500 MHz, δ in ppm, *J* in Hz. Data recorded in Dimethyl Sulfoxide-d_6.

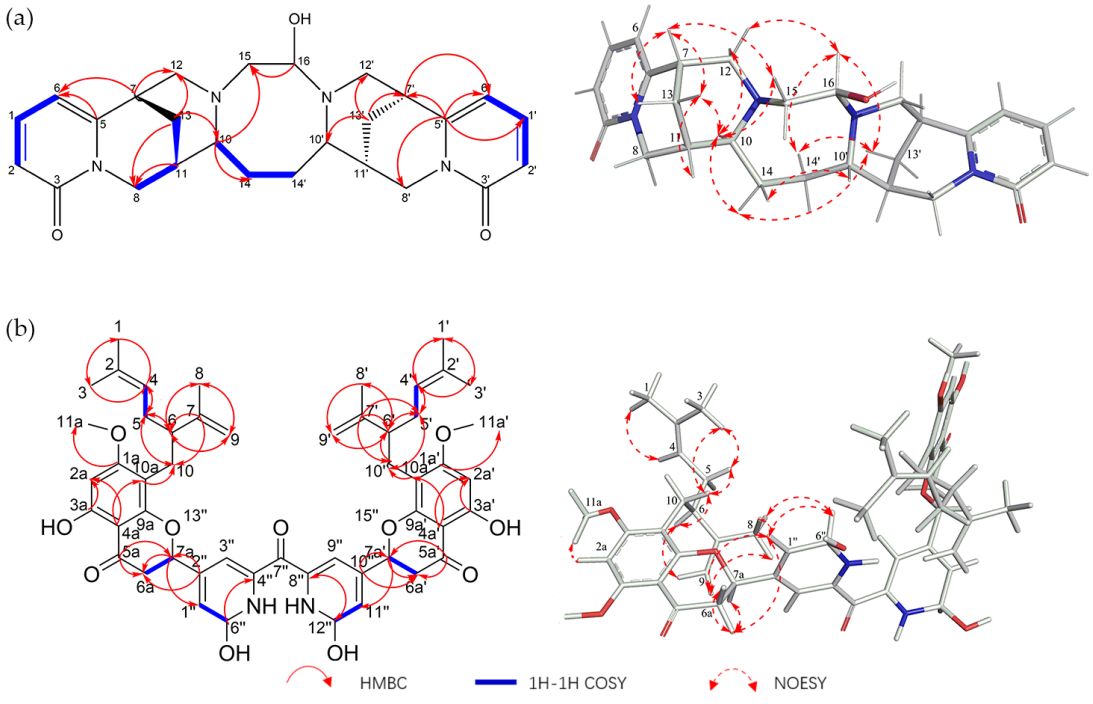

Figure 2. Key HMBC (arrows) and COSY (bold) and ROESY (arrows) correlations of **1** (a) and **2** (b)

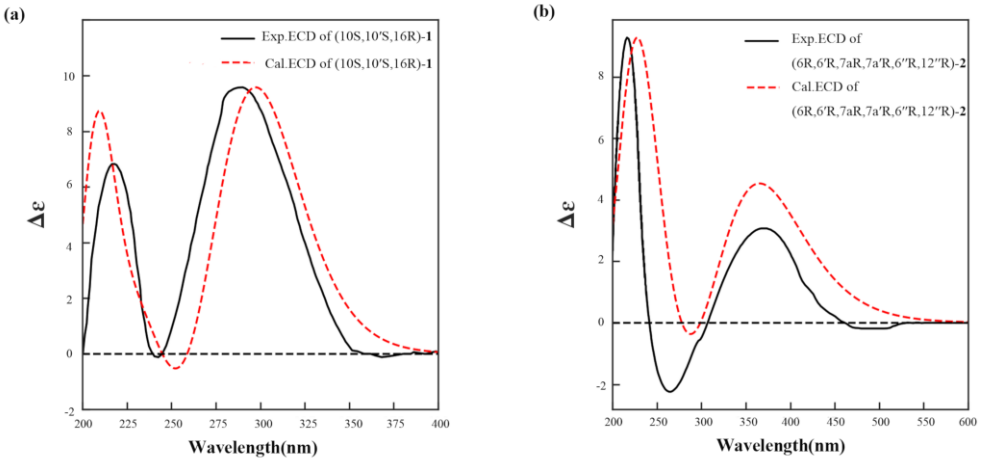

Figure 3. Experimental ECD and calculated ECD spectra of **1** (a) and **2** (b) in MeOH

Cytotoxicity assay The inhibitory effects that compound **1** and **2** had toward A431 and BT474 were investigated implementing an in *vitro* bioassay. Table 3 shows that the IC_{50} values of compound **2** to A431 and BT474 cells were 37.77 ± 0.98 and 38.13 ± 0.31 μM, respectively. Notably, lapatinib was used as a positive control in these experiments (IC_{50} = 15.07 ± 0.34 μM against A431 and IC_{50} = 0.16 ± 0.03 μM against BT474). Based on these results, comparing the IC_{50} values, sophobiflavanone (**2**) have moderate inhibitory activity on A431 and BT474.

Table 3. Inhibitory effect of Sophobikushenine and Sophobiflavanone on two human cancer cell lines (A431 and BT474).

IC_{50}: 50 % inhibitory concentration. (Mean ± SD of 3 tests)

Compound	IC_{50}(μM)	
	A431	BT474
1	>125	>125
2	37.77±0.98	38.13±0.31
Lapatinib	15.07±0.34	0.16±0.03

Cell scratch assay To analyze the effect of sophobiflavanone (**2**) on the metastasis of 4T1 cell migration, scratch assays were conducted for analyzing the effect of the compound on cell migration. The results indicated that the migration ability of sophobiflavanone-treated 4T1 cells was considerably lower than that of the control group. The scratch area of the control and sophobiflavanone groups at 24, 48, and 72 h

were narrower than their scratch widths at 0 h (Figure 4a), indicating that the 4T1 cells are constantly undergoing cell migration. By quantitatively calculating the cell migration rate, it was found that the 24 h and 72 h migration rates of the control group were 62.78% ± 2.90 and 94.67% ± 0.94, respectively, whereas the 24 h and 72 h migration rates of the sophobiflavanone-treated (30 μM) group were only 4.39% ± 0.74 and 6.28% ± 1.11, respectively (Figure 4b).

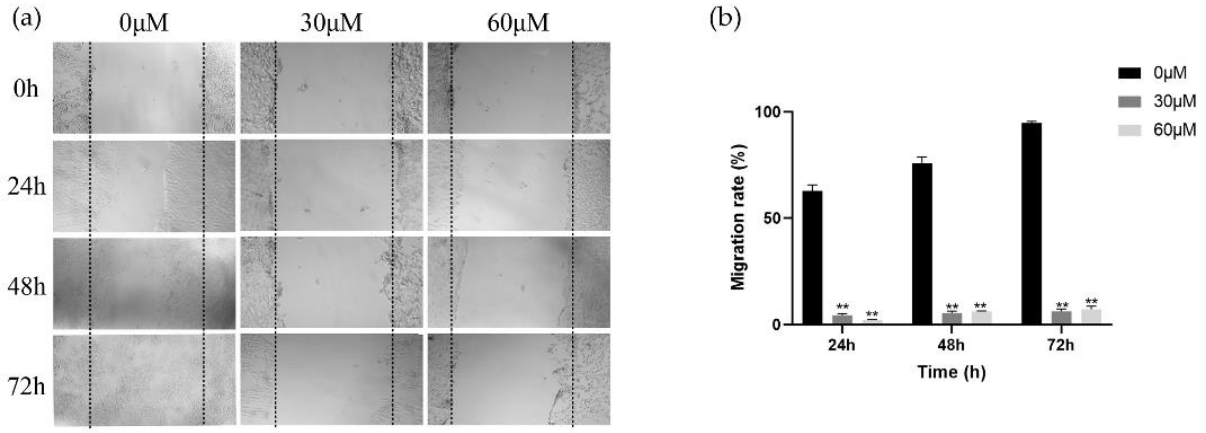

Figure 4. (a) Wounds were made by scraping a plastic tip across the cell monolayer and then 4T1 cells were treated with different concentrations of sophobiflavanone (0, 30 and 60 μM) and wound distances were imaged at 0, 24, 48 and 72 h. (b) The relative cell migration ability of sophobiflavanone was analyzed in the 4T1 cells. Results are representative of three independent experiments. **P <0.01 vs. the control at the same time-point.

EXPERIMENTAL

General Experimental Procedures IR spectra were measured by an IR spectrometer (Thermo Fisher Scientific, the United States). NMR spectra were performed on Bruker 500 MHz spectrometer (BioSpin, Switzerland), TMS was an internal standard. HR-ESI-MS were obtained on a Bruker solanX 70 FT-MS (Bruker BioSpin, Switzerland). Analytical HPLC data was carried out on Agilent 1260 infinity II instrument (Agilent Technologies, the United States) with an UV detector (Thermo Scientific dionex, the United States) and poroshell 120 EC-C18 column (5 μm, 4.6 mm × 150 mm, the United States). Preparative HPLC was given by a LC 3050N instrument with an UV detector (Beijing Chuangxintongheng Technology Co. Ltd., China) and an ODS-C18 column (250×20 mm, 5 μm, YMC Co. Ltd., Japan). UV spectra were measured by an Inesa L8 in MeOH (INESA Analytical Co. Ltd., China). ECD spectra were measured on JASCO J-815 spectrometers (JASCO Co. Ltd., Japan). Absorbance value of was carried on SPARK 10M (TECAN, Switzerland). The image was taken by 37XF light microscope

(Shanghai Optical Instrument Factory, China). Column chromatography (CC) was carried out with silica gel (200–300 mesh, Qingdao Waves Chemical Co. Ltd., China) and ODS-18 (S-50 μm, YMC Co. Ltd, Japan). Thin-layer chromatography (TLC) was acquired with TLC plates (Silica gel GF254, Qingdao Waves Chemical Co. Ltd., China). All the solvents were used in chemical grade (Shanghai Titan Technology Co. Ltd., China).

Plant materials The *Sophora flavescens* Ait. was collected in Sep 2020 from Zhengzhou City, Henan Province, P.R. China, and authenticated by Prof. Yong-Ming Luo, Jiangxi University of Chinese Medicine. A voucher specimen (SFA202009) was deposited at the Institute of New Drugs (Shanghai University of Engineering Science).

Extraction and isolation *Sophora flavescens* Ait. (60.0 kg) were crushed and extracted with 85% aq. EtOH (360 L, 3 h*3, each) at 75 ℃ to yield an extract (3.2 kg). The extract was dissolved in 1% $NH_3 \cdot H_2O$ to pH 10.0, and then partitioned with $CHCl_3$ until the $CHCl_3$ exact has no color reaction with potassium iodide reagent to afford a crude extract (520.0 g). On the basis of TLC and analytical HPLC analysis, four fractions, Frs. A–D was obtained with silica gel column chromatography ($CHCl_3$/MeOH, 15 cm×150 cm, 98:2, 95:5, 90:10, 70:30, 50:50, 30:70, v/v). Fr. B (55.0 g) was divided though ODS-18 column chromatography (MeOH/H_2O, 8×120 cm, 30:70, 50:50, 70:30, 100:0, v/v) into four fractions (Fr. B-1∼B-4). Sophobiflavanone (25.2 mg) was purified from Fr. B-3 (4.9 g) on ODS-18 column chromatography (3×50 cm, MeOH/H_2O 30:70, v/v). Fr. C (70.0 g) was divided on ODS-18 column chromatography (MeOH/H_2O, 8×120 cm,10:90, 30:70, 50:50, 70:30, 100:0, v/v) to obtain five subfractions (Fr.C-1∼C-5). Sophobikushenine (14.7 mg) was isolated from Fr. C-1(1.0 g) though semi-preparative HPLC (MeOH/H_2O 81:19, v/v, 3ml/min, tr=18.3 min).

Sophobikushenine (1) Yellow oil; $[\alpha]_D^{20}$ -217.4 (c 0.20, MeOH); HR-ESI-MS: *m/z* 471.2378 [M + Na] + (calcd for $C_{26}H_{32}N_4O_3Na$: 471.2372); UV λ_{Max}^{MeOH}: 321 nm, 291 nm, 236 nm; ECD (MeOH) λmax (Δε): 218 (+6.82), 290 (+9.57) nm; IR νmax 3413 cm^{-1}, 2928 cm^{-1},1646 cm^{-1} and 1584 cm^{-1};

Sophobiflavanone (2) Yellow amorphous powder; $[\alpha]_D^{20}$ +12.9 (c 0.19, MeOH); HR-ESI-MS: *m/z* 899.4101 [M + Na] + (calcd for $C_{51}H_{60}N_2O_{11}Na$: 899.4095); UV λ_{Max}^{MeOH}: 291 nm, 238 nm; ECD (MeOH) λmax (Δε): 216 (+9.28), 265 (−2.24), 372 (+3.07) nm; IR νmax 3338 cm^{-1},1599 cm^{-1},1499 cm^{-1} and 1459 cm^{-1}.

Cytotoxicity assay CCK-8 assay was used to indicated the cytotoxicity of sophobikushenine (**1**) and sophobiflavanone (**2**) against A431 and BT474. Lapatinib was used as a positive control drug. The cells were treated with various concentrations of the compounds for 72 h and the optical density (OD) was

detected as previously reported.[17] Microplate reader detects the absorbance value at 450 nm with Microplate reader. The cell viability was evaluated by percentage compared with DMSO (less than 0.05%) control group. The experiment was repeated 3 times to get the IC_{50} values.

Cell scratch assay Inhibition of sophobiflavanone (**2**) on cell migration was tested by cell scratch assay. 100 μL of 4T1 suspension was seeded onto 6-well plates at a density of $5x10^5$/well, and then cultured into monolayers. p100 pipette tip was used to make a scratch in the center of a 6-well plate. After removing the medium, the cells were rinsed 3 times with PBS in order to wash away cell debris. Sophobiflavanone (**2**) were diluted into different concentration (0, 30 and 60 μM) and added to the serum-free medium with which the cells cultured. The cell scratch area was imaged at 0, 24, 48 and 72 h, respectively though a light microscope at a magnification of x10. The cell scratch area at 0 h was used as the reference point. The cell invasion rate of the migration area was measured by Image J software. The experiment was repeated 3 times.

ACKNOWLEDGEMENTS

This work was supported financially by the National Natural Science Foundation of China (No. 81973453 and 81660652), Science and Technology Commission of Shanghai (No: 20DZ2255900)

REFERENCES

1. R. Huang, Y. Liu, L. L. Zhao, X. X. Chen, F. Wang, W. Cai, and L. Chen, *Nat. Prod. Res*., 2017, **31**, 2228.
2. L. Xia, A. Ztb, C. Li, and W. A. Cen, *J. Ethnopharmacol*., 2020, **269**, 113682.
3. M. Kuroyanagi, T. Arakawa, Y. Hirayama, and T. Hayashi, *J. Nat. Prod*., 1999, **62**, 1595.
4. J. Y. Ma, D. R. Zhao, T. Yang, D. Liu, R. T. Li, and H. M. Li, *Phytochem. Lett*., 2019, **29**, 138.
5. W. C. Huang, P. Y. Gu, L. W. Fang, Y. L. Huang, C. F. Lin, and C. J. Liou, *Phytomedicine*, 2019, **61**, 152852.
6. X. He, J. C. Fang, J. H. Huang, and X. Q. Wang, *J. Ethnopharmacol*., 2015, **172**, 10.
7. Y. B. Zhang, L. Q. Zhan, G. Q. Li, F. Wang, Y. Wang, Y. L. Li, W. C. Ye, and G. C. Wang, *J. Org. Chem*., 2016, **81**, 6273.
8. H. W. Yan, H. Zhu, X. Yuan, Y. N. Yang, Z. M. Feng, J. S. Jiang, and P. C. Zhang, *Bioorg. Chem*., 2019, **86**, 679.
9. M. Condello, E. Pellegrini, G. Multari, F. R. Gallo, and S. Meschini, *Toxicol. in Vitro*, 2020, **65**, 104819.
10. B. B. M. Hadden, *Anticancer Agents Med. Chem*., 2008, **8**, 807.

11. C. P. Wu, Y. Q. Li, T. H. Hung, Y. T. Chang, Y. H. Huang, and Y. S. Wu, *J. Nat. Prod*., 2021, **84**, 2544.
12. J. C. Wang, *Nat. Rev. Mol. Cell Biol.*, 2002, **3**, 430.
13. K. Asres, J. D. Phillipson, and P. Mascagni, *Phytochemistry*, 1986, **25**, 1449.
14. A. L. Sagen, J. Gertsch, R. Becker, J. Heilmann, and O. Sticher, *Phytochemistry*, 2002, **61**, 975.
15. H. Yamamoto, P. Zhao, and K. Inoue, *Phytochemistry*, 2002, **60**, 263.
16. S. Sato, J. Takeo, and C. Aoyama, *Bioorg. Med. Chem*., 2007, **15**, 3445.
17. T. E. Ali, M. A. Assiri, H. M. ElShaaer, S. M. Abed-Kariem, W. R. Abdel-Monem, S. M. El-Edfawy, N. M. Hassanin, A. A. Shati, M. Y. Alfaifi, and S. E. I. Elbehairi, *Heterocycles*, 2021, **102**, 1119.